

# Longitudinal Viscous Hydrodynamic Evolution for the Shattered Colour Glass Condensate

Akihiko Monnai<sup>1,\*</sup> and Tetsufumi Hirano<sup>1,†</sup>

<sup>1</sup>*Department of Physics, The University of Tokyo, Tokyo 113-0033, Japan*  
(Dated: March 6, 2022)

We investigate hydrodynamic evolution of the quark gluon plasma for the colour glass condensate type initial conditions. We solve full second-order viscous hydrodynamic equations in the longitudinal direction to find that non-boost invariant expansion leads to visible deformation on the initial rapidity distribution. The results indicate that hydrodynamic evolution with viscosity plays an important role in determining parameters for the initial distributions.

PACS numbers: 25.75.-q, 25.75.Nq, 12.38.Mh, 12.38.Qk

The heavy ion program at Large Hadron Collider (LHC) in European Organization for Nuclear Research (CERN) opens up new opportunities to explore the deconfined matter, the quark gluon plasma (QGP) [1], in a wider temperature region. There would be also a good opportunity to investigate the colour glass condensate (CGC) [2], *i.e.*, a universal form of colliding hadrons/nuclei at very high energies, of which we had a glimpse at Relativistic Heavy Ion Collider (RHIC) in Brookhaven National Laboratory (BNL) [3].

Heavy ion reactions at high energies undergo several stages such as collisions of two nuclei, local thermalisation, hydrodynamic evolution and chemical/thermal freeze-outs of the system. Since a framework to describe the CGC is regarded as an effective theory of high energy hadrons/nuclei, it is often employed to describe the very first stage in high energy heavy ion collisions and to calculate multiplicity and/or rapidity distributions without assuming secondary interactions [4–10]. Nevertheless, the data are remarkably described in this approach. On the other hand, relativistic hydrodynamic models are quite successful to describe space-time evolution of the QGP created in high energy heavy ion collisions, in particular, anisotropy of transverse collective flow [11–14]. Initial states of the hydrodynamic evolution, however, are still uncertain so that quantitative conclusion about transport coefficients depends on initial modeling [15]. This has been a longstanding issue which should be by all means resolved towards full understanding of the QGP. Both the initial gluon production from the CGC and the hydrodynamic evolution of the QGP are two distinct features of the whole reaction so that it is indispensable to unify these features [16] and to dynamically model the reactions as a whole from the colliding two nuclei to final observables in a comprehensive fashion.

A vast body of relativistic ideal and viscous hydrodynamic simulations have been performed so far to explore the bulk and transport properties of the QGP [17]. Boost

invariant expansion in the longitudinal direction [18] is, however, often assumed in most of these simulations to reduce the numerical efforts even though boost invariant rapidity distributions have never been observed. Since particle production in low transverse momentum region is dominated by the small  $x$  modes in the nuclear wave function, where  $x$  is a momentum fraction of incident partons, the QGP production could be traced back to the initial parton density at small  $x$  inside the colliding nuclei before collisions. The gluon density at small  $x$  rapidly increases with decreasing  $x$  and is eventually saturated due to non-linear interactions among gluons. The non-boost invariant gluon production is predicted within the  $k_T$ -factorisation formula as a consequence of  $x$  dependence of saturation scale,  $Q_s^2(x) \propto x^{-\lambda}$ , where  $\lambda \sim 0.3$  [2, 19] controls rapidity and collision energy dependences of the saturation scale.

In this Letter we describe hydrodynamic evolution of the hot matter in the beam direction with initial conditions from the shattered CGC. We focus especially on how hydrodynamic expansion with or without viscosity changes the flow-rapidity dependence of the entropy which could be identified with final rapidity distribution of hadrons. We neglect transverse hydrodynamic expansion in this study. Instead, we do not impose boost-invariance in the longitudinal expansion [20–22].

We solve the full second order constitutive equations [23] generalised from the ones in the Israel-Stewart theory [24] in the (1+1)-dimensional  $\tau$ - $\eta_s$  coordinates. Here  $\tau$  and  $\eta_s$  are the proper time and the space-time rapidity, respectively, defined as  $t = \tau \cosh \eta_s$  and  $z = \tau \sinh \eta_s$ . We neglect the baryon number current since we consider only gluon production in the  $k_T$ -factorisation formula as a initial condition. We choose the Landau frame where the energy dissipative current vanishes  $W^\mu = 0$ . Then the constitutive equations are

$$D\Pi = \frac{1}{\tau\Pi} \left( -\Pi - \zeta_{\Pi\Pi} \frac{1}{T} \nabla Y_f - \zeta_{\Pi\delta e} D \frac{1}{T} + \chi_{\Pi\Pi}^b \Pi D \frac{1}{T} + \chi_{\Pi\Pi}^c \Pi \nabla Y_f + \chi_{\Pi\pi} \pi \nabla Y_f \right), \quad (1)$$

\* monnai@nt.phys.s.u-tokyo.ac.jp

† hirano@phys.s.u-tokyo.ac.jp

$$D\pi = \frac{1}{\tau_\pi} \left( -\pi + \frac{4}{3}\eta\nabla Y_f + \chi_{\pi\pi}^b \pi D \frac{1}{T} + \chi_{\pi\pi}^c \pi \nabla Y_f + \frac{2}{3}\chi_{\pi\pi}^d \pi \nabla Y_f + \frac{2}{3}\chi_{\pi\Pi} \Pi \nabla Y_f \right), \quad (2)$$

where  $\Pi$  is the bulk pressure and  $\pi$  the shear pressure defined with the shear stress tensor  $\pi^{\mu\nu}$  as  $\pi = \pi^{00} - \pi^{33}$ . Note that, in the (1+1)-dimensional geometry, it is sufficient to treat  $\pi$  as the only independent component from the orthogonality and the traceless conditions.  $T$  is the temperature and  $Y_f$  is the flow rapidity defined by the four-fluid velocity  $u^\mu = (\cosh Y_f, 0, 0, \sinh Y_f)$ .  $\eta$  is the shear viscosity,  $\zeta_{\text{III}}$  and  $\zeta_{\text{II}\delta e}$  the bulk viscosities,  $\tau_\Pi$  and  $\tau_\pi$  the relaxation times and  $\chi_{\text{III}\pi}^b$ ,  $\chi_{\text{III}\pi}^c$ ,  $\chi_{\text{II}\pi}$ ,  $\chi_{\pi\pi}^b$ ,  $\chi_{\pi\pi}^c$ ,  $\chi_{\pi\pi}^d$  and  $\chi_{\pi\Pi}$  the second order transport coefficients. Here we have two ‘‘bulk viscosities’’,  $\zeta_{\text{III}}$  and  $\zeta_{\text{II}\delta e}$ , as required in the linear response theory. See also Ref. [23]. The time- and the space-like derivatives in this geometry are  $D = \cosh(Y_f - \eta_s)\partial_\tau + \frac{1}{\tau}\sinh(Y_f - \eta_s)\partial_{\eta_s}$  and  $\nabla = \sinh(Y_f - \eta_s)\partial_\tau + \frac{1}{\tau}\cosh(Y_f - \eta_s)\partial_{\eta_s}$ . Hydrodynamic equations become complicated in non-boost invariant case  $Y_f \neq \eta_s$  because derivatives with respect to the proper time and the space-time rapidity are mixed, which significantly increases the numerical difficulty compared with the constitutive equations in the transverse plane assuming the boost invariant flow.

We solve the constitutive equations (1) and (2) together with the energy-momentum conservation equations in the piecewise parabolic method [25] which was employed in one of the most successful (3+1)-dimensional ideal hydrodynamic calculations [13]. The numerical difficulty raised by the mixing of the derivatives with respect to  $\tau$  and  $\eta_s$  is dealt with by taking iteration on the expansion scalar  $\theta = \nabla Y_f$ . We have checked the solutions converge typically in several steps. Numerical details will be discussed elsewhere [26].

One needs the equation of state  $P_0 = P_0(e_0)$  and the transport coefficients, which contain microscopic information of the systems, to perform hydrodynamic simulations. We employ the latest (2+1)-flavor lattice QCD result [27] for the equation of state. On the other hand, we introduce some models for the transport coefficients since, to our knowledge, there is no single framework which gives all the transport coefficients appeared in this study. Here we use the conjectured minimum bound for the ratio of shear viscosity to the entropy density  $\eta/s = 1/4\pi$  from Anti-de Sitter/conformal field theory (AdS/CFT) correspondence [28] just for the purpose of demonstration to see how visible the entropy distribution changes during the longitudinal evolution. On the other hand, there are two bulk viscous coefficients  $\zeta_{\text{III}}$  and  $\zeta_{\text{II}\delta e}$  when the first-order cross terms are properly kept. So far there have been few calculations on these coefficients. Hence we try to get an insight for these two coefficients from the  $\phi^4$ -theory in the non-equilibrium statistical operator method [29] and calculate the ratios  $\zeta_{\text{III}}/\eta$  and  $\zeta_{\text{II}\delta e}/\eta$  as  $5T/6$  and  $-5T/2$ , respectively. Using the energy-momentum conservation and the Gibbs-

Duhem relation, the two linear terms are merged into one term at the first order as

$$-\zeta_{\text{III}} \frac{1}{T} \nabla_\mu u^\mu - \zeta_{\text{II}\delta e} D \frac{1}{T} = -\frac{\zeta_{\text{III}} + c_s^2 \zeta_{\text{II}\delta e}}{T} \nabla_\mu u^\mu, \quad (3)$$

where  $\zeta = (\zeta_{\text{III}} + c_s^2 \zeta_{\text{II}\delta e})/T = \frac{5}{2}(\frac{1}{3} - c_s^2)\eta$  corresponds to the conventional bulk viscous coefficient. The relaxation times  $\tau_\Pi$  and  $\tau_\pi$  and the other second order transport coefficients  $\chi_{\text{III}\pi}^b$ ,  $\chi_{\text{III}\pi}^c$ ,  $\chi_{\text{II}\pi}$ ,  $\chi_{\pi\pi}^b$ ,  $\chi_{\pi\pi}^c$ ,  $\chi_{\pi\pi}^d$  and  $\chi_{\pi\Pi}$  are estimated in kinetic theory as in Ref. [23]. The coefficients estimated with hadronic components up to  $\Delta(1232)$  are connected to those with  $u, d, s$  quarks and gluons as its components by hyperbolic factors around the (pseudo-)critical temperature as  $\chi = \frac{1}{2}(1 - \tanh \frac{T-T_0}{\Delta T})\chi_{\text{had}} + \frac{1}{2}(1 + \tanh \frac{T-T_0}{\Delta T})\chi_{\text{udsg}}$  where  $T_0 = 0.17$  GeV and  $\Delta T = 0.02$  GeV. The relaxation times are calculated likewise. We emphasize here that they are trial parameters to investigate qualitative response of the hot matter and that obtaining realistic transport coefficients is not the aim of this Letter.

The initial conditions for hydrodynamic simulations are obtained from Monte Carlo version [30] of  $k_T$ -factorisation formula with unintegrated gluon distributions parametrised by Kharzeev, Levin and Nardi (MC-KLN) [5, 31]. In this model the saturation scale  $Q_s$  for a nucleus  $A$  at a transverse coordinate  $\mathbf{x}_\perp$  is given as

$$Q_{s,A}^2(x; \mathbf{x}_\perp) = Q_{s,0}^2 \frac{T_A(\mathbf{x}_\perp)}{T_{A,0}} \left( \frac{x_0}{x} \right)^\lambda, \quad (4)$$

where  $T_A(\mathbf{x}_\perp)$  is a thickness function which is obtained from randomly distributed hard source (nucleons) according to the Woods-Saxon nuclear profile. We use the same parameter set,  $Q_{s,0}^2 = 2$  GeV<sup>2</sup>,  $T_{A,0} = 1.53$  fm<sup>-2</sup>,  $\lambda = 0.28$  and  $x_0 = 0.01$  as in Ref. [32]. The 5% most central events in the Monte-Carlo calculations are employed for constructing the smooth initial conditions. The initial energy density distribution as a function of space-time rapidity,  $e_0(\tau_0, \eta_s)$  is obtained from the transverse energy distribution  $dE_T/dy$  over the overlapping area of the nuclei  $S_{\text{area}}$  by identifying momentum rapidity  $y$  with space-time rapidity  $\eta_s$ . Although the pre-thermalisation stage would be very complicated, we simply assume, during a very short period until the thermalisation time  $\tau_0 = 1$  fm/c, the energy density in a fluid element at  $\tau_0$  is the same as locally deposited energy  $dE/d^2x_\perp \tau_0 d\eta_s$  calculated in the CGC. Maximum (minimum)  $p_T$  cut is set to 3 (0.1) GeV/c to include the contribution from low  $p_T$  partons which is assumed to form thermally-equilibrated media. When the saturation scale is smaller than  $\Lambda_{\text{QCD}}$ , we simply assume gluons are not produced in  $k_T$ -factorisation formula. This prescription leads to reduction of the gluon multiplicity at mid-rapidity by 21.5% at RHIC and 39.9% at LHC. The temperatures at mid-rapidity at the initial time are 419 MeV for RHIC and 490 MeV for LHC in these settings. We assume the boost-invariance only for the initial flow, *i.e.*,  $Y_f(\tau_0) = \eta_s$ , not for any other hydrodynamic initial

variables. It is more difficult to determine the initial conditions for the shear pressure  $\pi$  and the bulk pressure  $\Pi$  because the precise dynamics before the local thermalisation is not fully known. Here we set them to be vanishing since assuming finite dissipative currents at  $\tau_0$  corresponds to employing different initial energy-momentum tensors between ideal and viscous cases, which would make a comparison of the results and estimation of the viscous effects difficult.

We investigate the entropy distribution as a function of the flow rapidity  $dS/dY_f$  which roughly corresponds to the rapidity distribution of hadrons [33]. This can be interpreted as follows. The entropy density  $s$  carries the information of the number density in relativistic massless ideal gas limit since the ratio between the two quantities should be temperature independent as indicated by a dimensional analysis. Momentum rapidity  $y$ , on the other hand, can be identified with the flow rapidity  $Y_f$  in a fluid element on average. Thus, this is the closest quantity to the rapidity distribution we have from a pure hydrodynamic point of view, which do not include complicated freezeout processes nor any other model assumptions. Since the second order viscous correction to  $s^\mu$  should not be large, we discuss here the lowest order modification. One can make a rough estimation of charged particle rapidity density by  $dN_{\text{ch}}^{\text{hydro}}/dy \approx (2/3) \times (1/3.6) \times dS/dY_f$ .

The flow rapidity dependences of entropy are shown in Fig. 1 for Au+Au and Pb+Pb collisions at  $\sqrt{s_{NN}} = 200$  GeV and 2.76 TeV, respectively. The final times are  $\tau = 30$  fm/c and  $\tau = 50$  fm/c for the Au+Au and the Pb+Pb cases, respectively. These are the typical times at which the temperature at mid-rapidity is sufficiently close to the (pseudo-)critical temperature  $T_c \sim 0.17$  GeV. Note that they are much longer than a conventional lifetime of the QGP in the heavy ion collisions because the transverse expansion neglected in the present study would accelerate the cooling process.

One can see that the hydrodynamic evolution visibly modifies the initial distributions from the CGC model to more flattened ones at both RHIC and LHC energies. This behaviour can be seen only if boost-invariance is not assumed, *i.e.*, a pressure gradient with respect to  $\eta_s$  exists. Since entropy is produced in non-equilibrium hydrodynamic evolution, the entropy distributions are larger than those of the ideal hydrodynamic systems in most of the flow rapidity region. Final entropy at mid-flow rapidity results from the interplay between the entropy production and outward flow which carries entropy to the forward rapidity region. The ideal hydrodynamic process always lowers the yield of the initial distribution at mid-flow rapidity due to the outward flow. The viscous hydrodynamic one gives rather non-trivial results since the distribution is still lowered for the 200 GeV Au+Au collisions, but is enhanced for the 2.76 TeV Pb+Pb collisions. The difference is not due to the different choices of the final times, because, as we will see later, the shapes of the distributions do not change so much after  $\tau \sim 20$  fm/c for both cases. The modification of the initial distribution

is rather sensitive to the shape of the initial distribution. It should be noted that the corrections in the larger  $Y_f$  region ( $Y_f \gtrsim 3$  at RHIC and  $Y_f \gtrsim 6$  at LHC) might be slightly overestimated because even though the distribution shapes steady at a relatively early stage, the temperature in the forward region still hits  $T_c$  earlier than the mid-rapidity regions do and there would be additional hydrodynamic correction at the final times. This, of course, does not change the conclusion that the yield at the smaller rapidity regions are affected by hydrodynamic evolution. Considering that we use small shear and bulk viscous coefficients close to the conjectured minimum boundaries [28, 34] in the calculation, the results also suggest that effects of viscosity would be important. It should be noted that the numerical results here include only the longitudinal expansion and that the transverse expansion, which is missing in the present study, would be important in more quantitative discussion.

The fact that the initial entropy distribution  $dS/dY_f \approx dS/dy \propto dN/dy$  could be deformed during the hydrodynamic stage is of particular importance since initial gluon rapidity distribution is often directly compared with the observed charged hadron data assuming the parton-hadron duality [4–10]. As we saw above, the hydrodynamic expansion beyond the boost invariant flow could make a change of initial rapidity distribution. Thus, the  $\lambda$  parameter in some CGC-inspired models is subject to correction due to hydrodynamic effects if one wants to constrain it through the rapidity distribution. Even if one satisfactorily reproduced the rapidity distribution at RHIC with a set of CGC parameters assuming parton-hadron duality, one could fail to reproduce LHC data with the same parameter set due to lack of hydrodynamic corrections. Suppose the result from the viscous hydrodynamic model in Fig. 1 (a) would reproduce hadron rapidity distribution at RHIC, then the actual  $\lambda$  which includes the hydrodynamic expanding effects would be larger than an apparent  $\lambda$  which can be obtained by fitting this rapidity distribution without considering any secondary scatterings, as the distribution tends to become steeper as increasing  $\lambda$ . If one assumes that the hydrodynamic effect is smaller at LHC as indicated in Fig. 1 (b), this could be one of the possible interpretations for the fact that most of CGC models turned out to underpredict the multiplicity in the Pb+Pb collisions at LHC [35]. Since the entropy production due to viscosity is non-trivial as increasing collision energy, the energy dependence of multiplicity even at mid-rapidity from the CGC is also subject to hydrodynamic correction.

To further quantify the deviation from the boost invariance ( $Y_f = \eta_s$ ), we also estimate the difference between the flow rapidity and the space-time rapidity,  $Y_f - \eta_s$ . Results for Au+Au collisions at  $\sqrt{s_{NN}} = 200$  GeV and Pb+Pb collisions at  $\sqrt{s_{NN}} = 2.76$  TeV are shown up to the beam rapidities in Fig. 2. One sees in all cases that the deviations from the boost-invariant flow are positive and become large towards larger space-time rapidity due to the acceleration by the pressure gradient in the beam

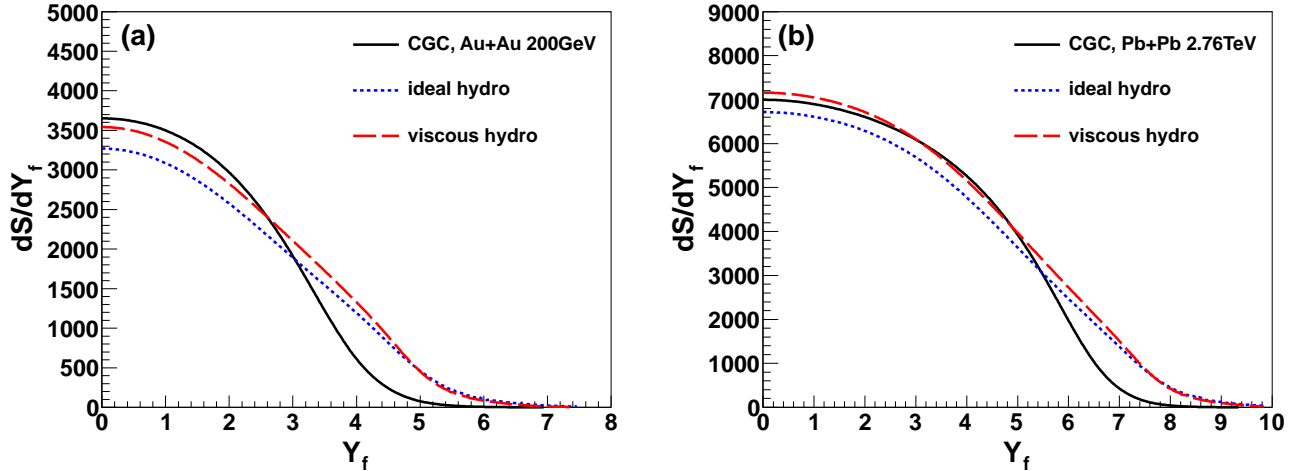


FIG. 1. (Colour online) The initial  $dS/dY_f$  distributions at  $\tau = 1$  fm/c from the colour glass condensate (solid line) and the final distributions after the ideal hydrodynamic (dotted line) and the shear and bulk viscous hydrodynamic (dashed line) evolution for (a) Au+Au collisions at RHIC ( $\tau = 30$  fm/c) and (b) Pb+Pb collisions at LHC ( $\tau = 50$  fm/c).

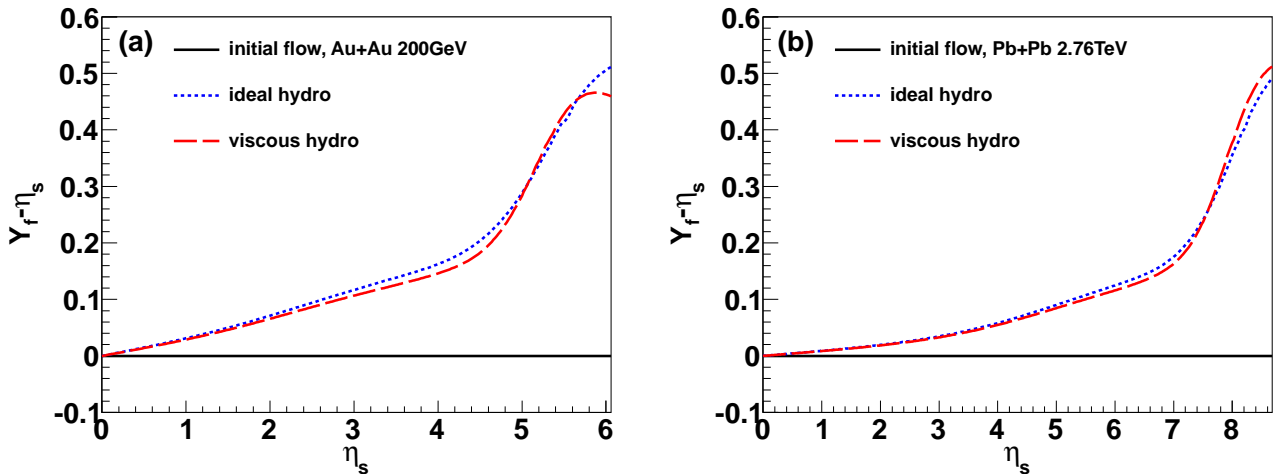


FIG. 2. (Colour online) The deviation of the flow rapidity from the space-time rapidity  $Y_f - \eta_s$  at the initial time  $\tau = 1$  fm/c (solid line) and after the ideal hydrodynamic (dotted line) and the shear and bulk viscous hydrodynamic (dashed line) evolution for (a) Au+Au collisions at RHIC ( $\tau = 30$  fm/c) and (b) Pb+Pb collisions at LHC ( $\tau = 50$  fm/c).

direction. Both Au+Au case at RHIC and Pb+Pb case at LHC exhibit the same trend, while the latter is slightly moderate near mid-rapidity possibly because initial energy density profile is less steep in the case. The deviations for the viscous cases are slightly smaller than those for the ideal cases for the  $Y_f$  regions in which the fluids are relatively hot, because the pressure gradients are effectively reduced in the longitudinal direction by the bulk and the shear pressures at early times in the space-time evolution. The situation, however, is different for the later times because the entropy generated in the viscous systems enhances the pressure gradients, while the corrections from the shear and the bulk pressures themselves are already small. Due to the counter contributions at

the late stage, the overall differences between the ideal and the viscous flow deviations are small at those proper times.

Finally, we demonstrate the time evolution of  $dS/dY_f$  and  $Y_f - \eta_s$  in Pb+Pb collisions at  $\sqrt{s_{NN}} = 2.76$  TeV. In Fig. 3 (a), the proper time dependence of the entropy distribution per flow rapidity is shown at the time  $\tau = 1, 5, 20$  and  $50$  fm/c. As mentioned earlier, the entropy distribution in the hydrodynamic evolution does not change much its shape after  $\tau \sim 20$  fm/c. The yield around  $Y_f = 0$  is almost constant throughout the time evolution. It is due to a rather accidental cancellation between the entropy production and the expansion by the outward entropy flux in the parameter settings. This means we

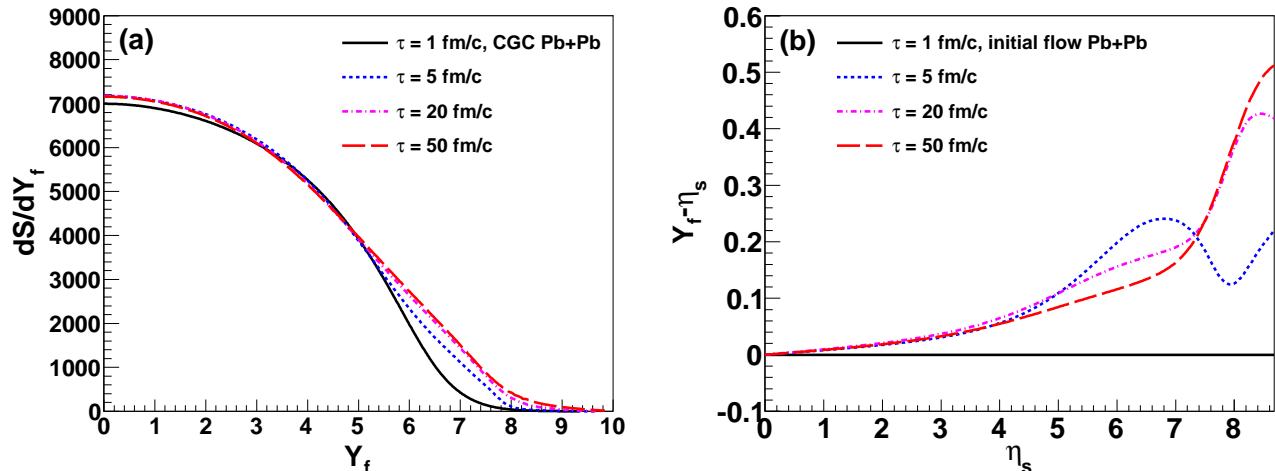


FIG. 3. (Colour online) (a) The deformation of the initial entropy distribution per flow rapidity and (b) the deviation of the flow rapidity from the space-time rapidity  $Y_f - \eta_s$  at initial time  $\tau = 1$  fm/c (solid line),  $\tau = 5$  fm/c (dotted line),  $\tau = 20$  fm/c (dash-dotted line) and  $\tau = 50$  fm/c (dashed line) in viscous hydrodynamic evolution in Pb+Pb collisions at the LHC energy.

have a monotonous decrease at mid-flow rapidity in the case of an ideal hydrodynamic calculation. In Fig. 3 (b), one sees the dynamical evolution of the deviation from the boost-invariant flow. At  $\tau = 5$  fm/c, there are a rise and a dip in the flow acceleration near  $Y_f \sim 6-7$  and  $7-8$ , respectively, because the effective pressure  $P_0 + \Pi - \pi$  can become very small in the large  $Y_f$  region when the absolute values of  $\Pi$  and  $\pi$  are still large. The sudden decrease in pressure leads to an enhancement in its gradient followed by a suppression. Note that the effect quickly disappears as the dissipative currents rapidly approach vanishing along with the time evolution. Eventually the flow rapidity distribution evolves into the one closer to the ideal hydrodynamic distribution we have seen in Fig. 2. It is worth-mentioning that, unlike  $dS/dY_f$ , the flow rapidity profile changes in the time evolution after  $\tau = 20$  fm/c for the current parameter sets.

To summarize, we developed a (1+1)-dimensional second-order viscous hydrodynamic model with both shear and bulk viscosity to see the QGP dynamics in the longitudinal direction. There is no boost-invariance at both RHIC and LHC energies in the CGC initial conditions, which causes the deformation of the entropy per flow rapidity. This indicates that the shapes of the (pseudo-)rapidity distributions of hadrons observed in experiments would reflect the initial gluon rapidity distri-

butions only indirectly due to the hydrodynamic evolution. This also motivates ones to correct the parameters, in particular,  $\lambda$  which controls the rapidity dependence of entropy production, in the initial conditions. While the precise determination of the parameters should be left to a (3+1)-dimensional viscous hydrodynamic calculation, our current parameter settings suggest that a conventional  $\lambda$  which is determined without the hydrodynamic effect would be smaller than the true  $\lambda$  at RHIC but is not so much different at LHC around the mid-rapidity region. This could play an important role in explaining the gap between the CGC predictions of multiplicity based on RHIC data and the latest experimental data at LHC [35]. In future, more realistic wave functions under running-coupling quantum evolution will be employed [36]. We will discuss parameter dependences and numerical aspects in detail in near future [26].

## ACKNOWLEDGMENTS

The authors acknowledge fruitful discussion with Y. Nara. The work of A.M. was supported by JSPS Research Fellowships for Young Scientists. The work of T.H. was partly supported by Grant-in-Aid for Scientific Research No. 22740151.

- 
- [1] K. Yagi, T. Hatsuda and Y. Miake, *Camb. Monogr. Part. Phys. Nucl. Phys. Cosmol.* **23** (2005) 1.  
[2] F. Gelis, E. Iancu, J. Jalilian-Marian and R. Venugopalan, arXiv:1002.0333 [hep-ph].  
[3] J. P. Blaizot and F. Gelis, *Nucl. Phys. A* **750** (2005) 148.

- [4] D. Kharzeev and M. Nardi, *Phys. Lett. B* **507** (2001) 121.  
[5] D. Kharzeev and E. Levin, *Phys. Lett. B* **523** (2001) 79.  
[6] D. Kharzeev, E. Levin and M. Nardi, *Phys. Rev. C* **71** (2005) 054903.

- [7] D. Kharzeev, E. Levin and M. Nardi, Nucl. Phys. A **747** (2005) 609.
- [8] J. L. Albacete, Phys. Rev. Lett. **99** (2007) 262301.
- [9] E. Levin and A. H. Rezaeian, Phys. Rev. D **82** (2010) 054003;  
E. Levin and A. H. Rezaeian, arXiv:1011.3591 [hep-ph];  
E. Levin and A. H. Rezaeian, arXiv:1102.2385 [hep-ph].
- [10] L. McLerran and M. Praszalowicz, Acta Phys. Polon. B **41** (2010) 1917.
- [11] P. F. Kolb, P. Huovinen, U. W. Heinz and H. Heiselberg, Phys. Lett. B **500** (2001) 232;  
P. Huovinen, P. F. Kolb, U. W. Heinz, P. V. Ruuskanen and S. A. Voloshin, Phys. Lett. B **503** (2001) 58;  
P. F. Kolb, U. W. Heinz, P. Huovinen, K. J. Eskola and K. Tuominen, Nucl. Phys. A **696** (2001) 197.
- [12] D. Teaney, J. Lauret, and E. V. Shuryak, Phys. Rev. Lett. **86** (2001) 4783.
- [13] T. Hirano, Phys. Rev. C **65** (2002) 011901.
- [14] T. Hirano and K. Tsuda, Phys. Rev. C **66** (2002) 054905.
- [15] H. Song, S. A. Bass, U. W. Heinz, T. Hirano and C. Shen, arXiv:1011.2783 [nucl-th].
- [16] T. Hirano and Y. Nara, Nucl. Phys. A **743** (2004) 305.
- [17] P. Huovinen and P. V. Ruuskanen, Ann. Rev. Nucl. Part. Sci. **56**, (2006) 163;  
T. Hirano, N. van der Kolk and A. Bilandzic, arXiv:0808.2684 [nucl-th];  
U. W. Heinz, arXiv:0901.4355 [nucl-th];  
P. Romatschke, arXiv:0902.3663 [hep-ph];  
D. A. Teaney, arXiv:0905.2433 [nucl-th].
- [18] J. D. Bjorken, Phys. Rev. D **27** (1983) 140.
- [19] K. Golec-Biernat and M. Wusthoff, Phys. Rev. D **59** (1999) 014017;  
K. Golec-Biernat and M. Wusthoff, Phys. Rev. D **60** (1999) 114023.
- [20] M. C. Chu, Phys. Rev. D **34** (1986) 2764.
- [21] Y. Akase, S. Daté, M. Mizutani, S. Muroya, M. Namiki and M. Yasuda, Prog. Theor. Phys. **82** (1989) 591.
- [22] P. Bozek, Phys. Rev. C **77** (2008) 034911.
- [23] A. Monnai and T. Hirano, Nucl. Phys. A **847** (2010) 283;  
A. Monnai and T. Hirano, J. Phys.: Conf. Ser. **270** (2011) 012042.
- [24] W. Israel and J. M. Stewart, Annals Phys. **118** (1979) 341.
- [25] P. Colella and P. R. Woodward, J. Comp. Phys. **54** (1984) 174.
- [26] A. Monnai and T. Hirano, in preparation.
- [27] S. Borsanyi *et al.*, JHEP **1011** (2010) 077.
- [28] P. Kovtun, D. T. Son, and A. O. Starinets, Phys. Rev. Lett. **94** (2005) 111601.
- [29] A. Hosoya, M. a. Sakagami, and M. Takao, Annals Phys. **154** (1984) 229.
- [30] H. J. Drescher and Y. Nara, Phys. Rev. C **75** (2007) 034905;  
H. J. Drescher and Y. Nara, Phys. Rev. C **76** (2007) 041903.
- [31] D. Kharzeev, E. Levin and M. Nardi, Nucl. Phys. A **730** (2004) 448 [Erratum-ibid. A **743** (2004) 329].
- [32] T. Hirano and Y. Nara, Phys. Rev. C **79** (2009) 064904.
- [33] K. Morita, S. Muroya, C. Nonaka and T. Hirano, Phys. Rev. C **66** (2002) 054904.
- [34] A. Buchel, Phys. Lett. B **663** (2008) 286.
- [35] K. Aamodt *et al.* [The ALICE Collaboration], Phys. Rev. Lett. **105** (2010) 252301.
- [36] J. L. Albacete and A. Dumitru, arXiv:1011.5161 [hep-ph].